

(22) Iron-Based Mixed Metal Carbide Fischer-Tropsch Catalysts

This three-year effort will seek to develop a more active, selective, attrition resistant and stable Fe FTS catalysts based on formulations containing a second metal (besides Cu) capable of forming mixed metal carbides with Fe.

Total project cost: \$1,334,594

Funding request: \$875,499

Project Lead: Clemson University

Project Participants: Louisiana State University; RTI; Rentech; Sud-Chemie, Inc.; South Carolina Energy Office; Louisiana State Energy Office

Start Date: August 31, 2005

End Date: August 31, 2008

Public Abstract

"Iron-Based Mixed Metal Carbide Fischer-Tropsch Catalysts"

Research is being carried out that addresses the need for highly active, selective, attrition resistant and stable iron-based catalysts for converting low H₂/CO ratio syngas from coal and biomass to clean fuels, additives, and lubricants using the Fischer-Tropsch synthesis (FTS). The 36-month research project involves **Clemson University** (the prime contractor, a state university in South Carolina), **Louisiana State University** (a state university in Louisiana), **RTI** (a non-profit research institution in North Carolina), **Süd-Chemie Inc.** (a private company in Kentucky), **Rentech** (a private company in Colorado), the **South Carolina State Energy Office**, and the **Louisiana State Energy Office**.

Gasification followed by FTS is currently the most promising method for upgrading low-value coal and biomass to high-value liquid fuels and chemicals. There are sufficient domestic reserves of coal to supply most of US fuel needs for more than one hundred years using FTS. Because biomass is formed by fixation of atmospheric CO₂, its use as a fuel feedstock is attractive because this results in virtually no net CO₂ emissions. The total biomass produced each year as waste material from agriculture and forest operations could be converted into roughly 40 billion gal/yr of liquid fuel, roughly 25% of the current US gasoline usage.

Bulk iron (Fe) catalysts are the catalysts of choice for converting low H₂/CO ratio syngas to fuels via FTS. These relatively low-cost catalysts have low methane selectivity and high water gas shift activity (which generates H₂ *in situ*). However, development of a bulk Fe FTS catalyst that combines high FT activity, low methane selectivity, high attrition resistance (i.e., ability to withstand physical breakage), and long-term stability (low deactivation rate) is still elusive and presents a widely recognized barrier to the commercial deployment of FTS for coal and biomass conversion. The critical property determining the activity and deactivation of Fe catalysts for FTS appears not to be Fe in the metallic state but the carburized Fe surface.

This research project addresses the issues of the nature, the genesis, and the maintenance of active Fe sites from a totally different perspective than previous studies. Unlike previous studies of Fe bimetallic catalysts, this work focuses on the ability of second and third metals to form mixed-metal carbides with Fe at reaction or pretreatment conditions. Improvements in activity should result as catalytically active surface carbide structures are stabilized in the presence of H₂O and CO₂, important for use at the high conversions required for commercial operation. This should also result in a decrease in the rate of deactivation, thereby improving the longevity of the catalyst. Interesting selectivities, especially low methane production, should result as we modify the nature of the active surface carbide and, potentially, the active sites. The

catalysts synthesized will be studied using Fischer-Tropsch synthesis (high pressure gas phase, steady-state isotopic transient kinetic analysis, slurry phase including with a slurry bubble column reactor) and detailed characterization (x-ray absorption fine structure, x-ray diffraction, chemisorption, attrition testing, among others). The results from the various studies compared to the benchmark catalyst will then be used to evaluate commercial potential.

1.0 Statement of Project Objectives

The objective of the research project is to develop more active, selective, attrition resistant and stable Fe FTS catalysts based on formulations containing a second metal (besides Cu) capable of forming mixed metal carbides with Fe. The research addresses the issues of the nature, the genesis, and the maintenance of active Fe sites from essentially a totally different perspective than previous studies. Contrary to previous studies of Fe bimetallic catalysts, this work focuses on the ability of the second metal to form mixed-metal carbides with Fe at reaction or pretreatment conditions rather than on the alloying properties of the 2 metals. Improvements in activity should result as we better stabilize catalytically active surface carbide structures in the presence of H₂O and CO₂, important for use at the high conversions required for commercial operation. This should also result in a decrease in the rate of deactivation, thereby improving the longevity of the catalyst. Interesting selectivities, especially low methane production, may result as we modify the nature of the active surface carbide and, potentially, the active sites. The catalysts will be prepared, using methodology developed by members of the team at RTI and Clemson, to be attrition resistant so that they can be used in slurry phase reaction in an SBCR.

2.0 Project Activities

Project activities are progressing in accordance with the project schedule (Table 1). During this 7th quarter of activities the main focus has been on preparing Fe catalysts with K and Mn addition by varying %loading and on studying their catalytic activities. These activities are described in the following section comprising the experimental methodology and results.

Table 1: Project Schedule

Tasks	Activity											
	Year 1				Year 2				Year 3			
	1	2	3	4	1	2	3	4	1	2	3	4
Task 1: Catalyst Prep.	X	X	X		X		X		X		X	
Task 2: Catalyst Charac.	X	X	X	X	X	X	X	X	X	X	X	
Task 3: Reaction Study		X	X	X	X	X	X	X	X	X	X	X
Task 4: Slurry Phase Reactor Testing			X	X			X	X		X	X	
Task 5: Eval. of Comm. Potential					X				X			X

2.1 Methodology

2.1.1 Catalyst Preparation

Catalysts were prepared according to the general formulation, $(100-x)\text{Fe}/x\text{Mn}/5\text{Cu}/17\text{Si}$ where x is 20 or smaller, using the constant pH precipitation technique [1]. First, $\text{Fe}(\text{NO}_3)_3 \cdot 9\text{H}_2\text{O}$ (~0.6 M) and $\text{CuN}_2\text{O}_6 \cdot 3\text{H}_2\text{O}$ were added together into 40 ml of H_2O while $\text{Mn}(\text{NO}_3)_2$ was added into 20 ml of H_2O . Tetraethylorthosilicate ($\text{Si}(\text{OC}_2\text{H}_5)_4$, TEOS) was added into 40 ml of propanol. Then the solutions were mixed together and heated to $83 \pm 3^\circ\text{C}$. In the same time, NH_4OH (~2.7 M) was heated to $83 \pm 3^\circ\text{C}$. After reaching 83°C , aqueous NH_4OH was slowly added into the mixed solution containing Fe, Cu, Si and Mn precursors under vigorous stirring until the solution was precipitated and pH was 8-9. The precipitate was aged in a vessel at room temperature for 17 h and thoroughly washed with deionized water to remove excess NH_3 to obtain the pH of 7-8 (1.3-1.5 liters of deionized water used). The washed precipitate was dried in an oven for 18-24 h at 110°C and was sieved $< 90 \mu\text{m}$. The catalyst precursor was calcined in static air at 300°C for 5 h, and then cooled to room temperature over a 2-h period in a muffle furnace. In the case of K promotion, the resulting catalysts after sieving were impregnated to incipient wetness with KHCO_3 solution to give the desired K concentration. Subsequently, the catalyst was dried in the oven over 4 h prior to calcination.

2.1.2 Catalyst Characterization

Catalysts were characterized by elemental analysis, N_2 adsorption (BET, pore volume, pore size distribution), XRD (Fe and *Me* crystalline phases formed), and CO pulse chemisorption (surface metal atoms), and EXAFS (the structure and coordination of Fe atom).

a) Elemental Analysis

Elemental analysis is performed to determine the composition of elements in the bulk of catalysts. The composition content of catalysts is determined using ICP-OES at Galbraith Laboratories.

b) N_2 Adsorption

The BET surface area, pore volume, average pore diameter, and pore size distribution of the catalysts are determined by N_2 physisorption using a Micromeritics ASAP 2010 automated system. A 0.3 g catalyst sample is degassed in the Micromeritics ASAP 2010 at 100°C for 1 h and then at 300°C for 2 h with $10^\circ\text{C}/\text{min}$ ramping rate prior to analysis. The analysis is done using N_2 adsorption at -196°C .

c) X-Ray Diffraction (XRD)

XRD is used to determine the phase composition of Fe catalysts as prepared and after pretreatments. The XRD spectrum of the catalysts is collected using an X-ray diffractometer, Scintag 2000 x-ray diffractometer, using monochromatized $\text{Cu K}\alpha$ radiation (40 kV, 40 mA) and a Ge detector using a step scan mode at a scan rate of $0.02^\circ (2\theta)$ per second from 10 - 80° . XRD peak identification is done by comparison to the JCPDS database software.

d) CO-Pulse Chemisorption

Fe dispersion is determined by pulsing CO over the reduced catalyst.

Approximately 0.2 g of catalyst is put in a quartz tube, incorporated in a temperature-controlled oven and connected to a thermal conductivity detector (TCD). He is used as a carrier gas for this system. Prior to chemisorption, the catalyst is reduced in a flow of hydrogen (50 cc/min) at 280°C for 12 h.

Afterwards, the sample is cooled down to 35°C with He 30cc/min. CO is pulsed at 35°C over the reduced catalyst until the TCD signal is constant. An assumed stoichiometry ratio on the surface of $\text{CO}:\text{Fe}_s^0 = 1:2$ is used [2].

e) Extended X-ray absorption fine structure (EXAFS)

EXAFS is used to provide information on the structure and coordination of atoms on the catalyst surface. The catalysts are studied at the Center for Advanced Microstructures and Devices (CAMD) at LSU.

2.1.3 CO Hydrogenation Reaction Studies

CO hydrogenation is performed using 0.1 g of catalyst packed in a fixed bed-quartz reactor with i.d. = 8 mm. The total flow rate used is 60 cc/min with the H_2/CO ratio of 2/1 in a balance of He. The catalyst sample is pretreated in 30 cc/min of H_2 at 280°C for 12 h with 2°C/min ramping rate prior to CO hydrogenation.

CO hydrogenation reactions are carried out at 280°C and at 1.8 atm. The product streams are analyzed by gas chromatography.

2.2 Results and Discussion

During this quarter, we have completed TPR and CO chemisorption results for catalyst characterization of the catalysts with 5 mol% of various third transition metals. We have found that the heating rate used during TPR has an impact on the catalyst reduction behavior. TPR results reported in the 6th quarterly report were obtained using a heating rate of 5°C/min which was different from that used to reduce catalysts prior to reaction (2°C/min). Therefore, TPR was carried out again using a heating rate of 2°C/min in order to obtain the reduction behavior of catalysts under a similar condition to catalyst pretreatment. Samples were held at 280°C for 12 h and then the temperature was ramped up to 800°C.

A TPR profile of 100Fe is plotted against the reduction time in Fig. 1. No significant amount of H_2 was consumed, although the sample was held at 280°C for 12 h. On the other hand, the 2nd reduction was detected after temperature was ramped up from 280-850°C. Therefore, as was done, only the first reduction peak should account for the reduction of Fe under the reduction condition used for the catalyst pretreatment. This way, results shown in Table 2 do not include %Fe reducibility arising from the second peak. Typical TPR profiles for all catalysts are shown in Fig. 2. For comparison purposes, a pure Fe_2O_3 powder was included as reference.

Unfortunately, all Fe catalysts as prepared in this study were XRD amorphous.

Therefore, we could not ascertain phases of Fe present. However, it is reasonable to assume that only the Fe_2O_3 phase was present after calcination based on the similar TPR profiles for all prepared Fe catalysts and pure Fe_2O_3 powder.

Comparing the TPR profiles of the as prepared Fe catalysts and pure Fe_2O_3 powder (Fig. 2), it clearly shows that adding Cu facilitates the reducibility of Fe as expected, by which the peaks in the TPR profiles were shifted to a lower reduction temperature for all samples.

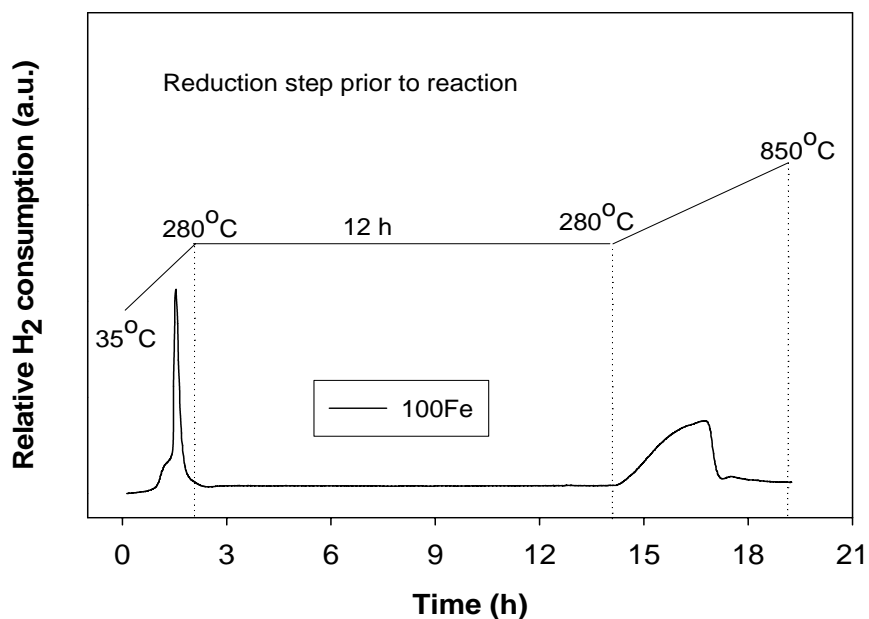


Figure 1: A comparison of TPR profile of 100Fe with reduction time and temperatures.

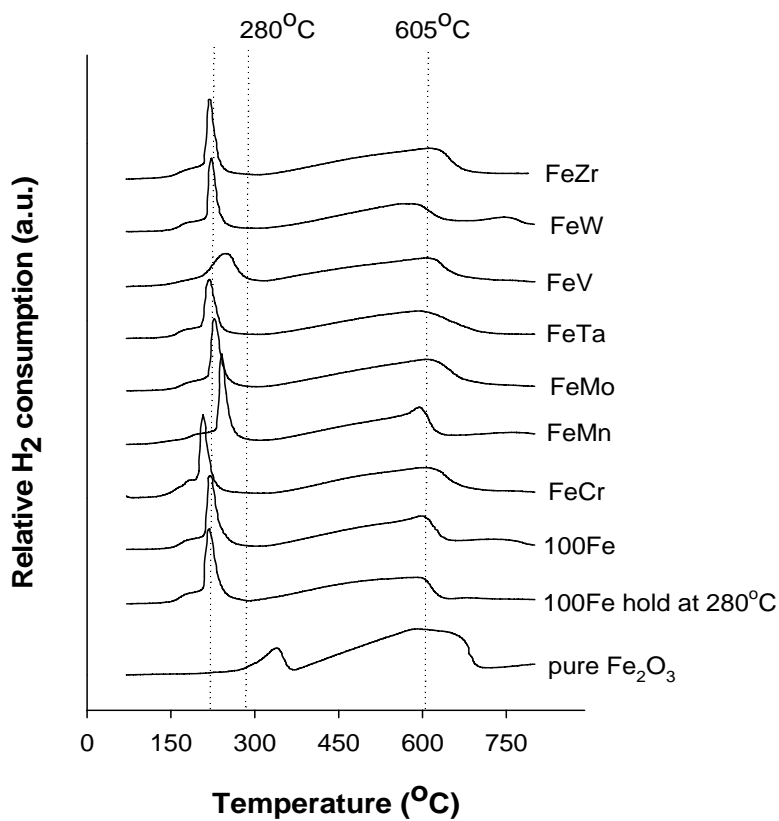


Figure 2: TPR profiles of the fresh calcined Fe-based catalysts.

Fig. 2 reveals that all catalysts showed 2 distinct peaks at temperatures of approx. 215°C for the first peak and 600°C for the second peak. It has been suggested that the reduction of Fe₂O₃ occurs via 2 main steps: Fe₂O₃ → Fe₃O₄ → Fe. These 2 elementary reactions have been assigned to the first and second peaks in the TPR profiles, respectively [3,4]. However, it is likely that some of Fe₂O₃ could be reduced to Fe₃O₄ and further Fe rapidly. Thus, the calculation of %reducibility of Fe accounted for the first peak was done on the basis of Fe₂O₃ → Fe.

As shown in Table 2, peak temperatures and the reducibility of Fe varied depending upon type of added metal. Not all of the third metals enhanced the reducibility of Fe. Therefore, %Fe reducibility could be categorized into 2 groups; high (51-57 % for 100Fe, FeCr, FeMn, FeMo and FeZr) and low (40-48 % for FeTa, FeV and FeW), using the unpromoted 100Fe catalyst as a reference. It appears that the promotion of Fe catalyst with a third metal did not increase the reducibility of Fe with the exception in the case of Mn. FeMn showed the highest %Fe reducibility (57%) but the reduction peak temperature was delayed to 241°C. It has been suggested by Lee et al. [5] that MnO can stabilize Fe²⁺, thus delaying the reduction of Fe³⁺ to Fe⁰ to a higher reduction temperature.

Table 2: Results from TPR and CO-Chemisorption of various Fe-based catalysts.

Catalyst ^a	H ₂ -TPR		CO-Chemisorption		
	Peak temperature (°C) ^b	%Fe Reducibility ^c	%Fe Dispersion ^d	Total chemisorbed CO (□mol/g) ^e	d _p ^f (nm)
100Fe	215	53	2.5	116	30
FeCr	207	51	5.7	252	13
FeMn	241	57	3.9	155	20
FeMo	228	53	3.6	148	21
FeTa	215	48	3.4	139	22
FeV	249	40	3.8	157	20
FeW	222	47	2.6	107	29
FeZr	215	51	3.8	169	20

^a Containing 5Cu and 17Si.

^b Max error = $\pm 5^{\circ}\text{C}$

^c %Fe reduced under the reaction reduction (hold at 280°C for 12h). Max error = $\pm 5\%$.

^d %Dispersion = amount of surface-exposed $\text{Fe}^0 \times 100$ / total number of Fe atoms.

^e Determined by extrapolating the total volume adsorption isotherm to zero pressure.

Max error $\pm 4\%$.

^f The average Fe particle size (d_p) = $0.75 / \text{Fe Dispersion}$ where Fe site density was assumed to be $0.094 \text{ nm}^2 / \text{Fe atom}$ [6].

On the other hand, a lower %reducibility of Fe was observed for FeTa, FeV and FeW catalysts. FeV showed the lowest %Fe reducibility (40%) and the peak temperature was delayed about 34°C with respect to that of the 100Fe catalyst. It was reported by Junior et al. [7] that V can distribute in the Fe oxide structure which could result in a higher reduction temperature and less amount of Fe reduced. In contrast, the addition of Mo did not show any impact on the reducibility of Fe, resulting in relatively the same value as the benchmark 100Fe catalyst, although the study of Ma et al. [8] has shown that Fe supported on activated carbon catalyst was less reduced when Mo was added. The divergence in results could have been due to a difference in catalyst composition.

Table 2 also shows %Fe dispersion, amount of total CO chemisorbed and the average particle size of metallic Fe. The average Fe^0 particle size was calculated based upon 0.094 nm^2 of Fe site density/Fe atom [6]. %Dispersion and the average Fe^0 particle size of 100Fe were 2.5% and 30 nm, respectively. For all third metal promoted catalysts (except W), these values were in the range of 3.4-5.7 % and 13-22 nm. Thus, adding a third metal promoted the dispersion of Fe and reduced the average particle size of Fe by 40% and 33%, respectively. The

only exception was the catalyst containing W where the dispersion of Fe was not improved showing relatively the same value as the benchmark 100Fe catalyst. The catalyst with Cr addition exhibited the highest %Fe dispersion (5.7%), and consequently the smallest average Fe⁰ particle size (13 nm). It could be postulated that Cr was able to prevent Fe particles from sintering and stabilized small metallic Fe particles.

A summary of reaction rate and TOF_{chem} for the FeMe catalysts and the benchmark catalyst are reported in Table 3. The activity of catalyst at the maximum was used to calculate TOF_{chem}. Table 3 suggests that the higher activity observed for FeMn and FeZr samples was due to higher TOF_{chem} values (0.011 – 0.013 s⁻¹) rather than a higher density of active sites. Hence, adding Mn and Zr gave rise to stronger active sites while Cr promotion resulted in a greater number of sites that are active for the reaction (determined using CO chemisorption) due to the better %Fe dispersion.

Table 3: Variations in activity of Fe catalyst and TOF.

Catalyst ^a	Max rate ^b (□mol of carbon/g/s)		SS rate ^b (□mol of carbon/g/s)		TOF _{chem} ^c (s ⁻¹) x 10 ³
	CO ₂	total HC	CO ₂	total HC	
100Fe	0.50	0.36	0.13	0.22	7.4
FeCr	1.14	0.85	0.25	0.27	7.9
FeMn	0.99	0.76	0.24	0.34	11.3
FeMo	0.64	0.46	0.19	0.21	7.4
FeTa	0.61	0.53	0.12	0.21	8.2
FeV	0.76	0.58	0.21	0.26	8.5
FeW	0.25	0.33	0.11	0.18	5.4
FeZr	1.27	0.93	0.24	0.32	13.0

^a Containing 5Cu and 17Si.

^b Max error = ± 2%.

^c Calculated from TOF_{chem} = reaction rate (at the maximum activity)/amount chemisorbed CO. Max error ± 3%

^d Based on atomic carbon.

During this period, at LSU, Fe₃C was synthesized for using as a XANES “fingerprint analysis” by treating Fe₂O₃ and in a CO temperature programmed reduction environment using an Altamira Instruments® AMI-1, following the procedure shown in Fig. 3 [9,10]. TPR with CO was followed by cooling in He and passivation at room temperature (10:1 ratio of He: 90 He/10 O₂, 50 cc/min, 20 min). Carbon is an interstitial impurity in the Fe lattice [11]; thus, if the carbide phase forms (in the absence of a high temperature-oxidizing environment), carbon will retain the metallic iron oxidation state. Therefore, a comparison of XANES for synthesized Fe₃C and Fe foil (Fe⁰) was used and the data are shown in Figures 4 and 5. It clearly suggests the formation of Fe₃C as the oxidation state for Fe₃C coincides with that of the Fe foil (7.5 nm thick), using the derivative of the XANES (the maximum being a pseudo electron binding energy [12,13] (Figure 5).

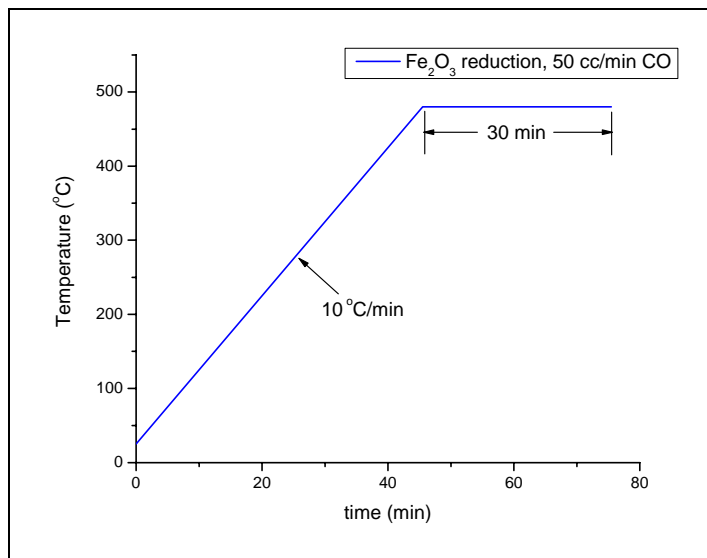


Figure 3: TPR temperature profile for Fe₂O₃ + CO

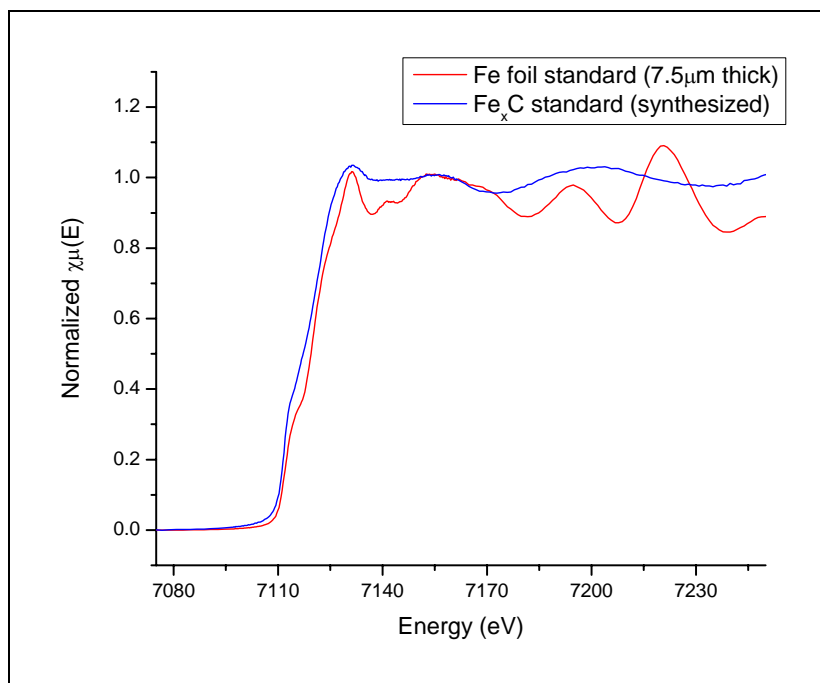


Figure 4: Normalized XANES spectrum of Fe foil, Fe_xC standards

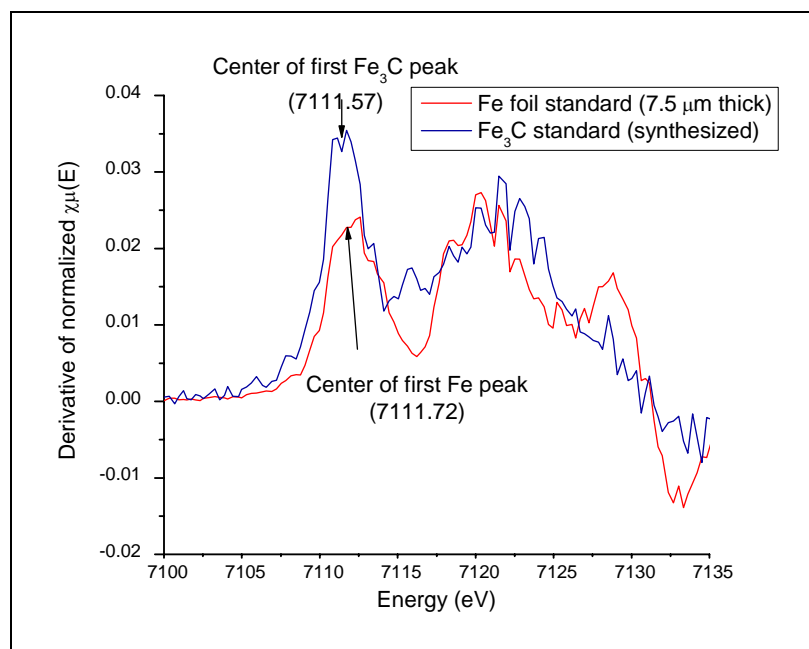


Figure 5: Derivative of normalized XANES region for Fe foil, Fe_xC

As shown in the previous report, the activity of the Fe catalyst was most enhanced by the addition of Mn and was not altered by the addition of K. Therefore, XANES was carried out on various Fe catalysts containing Mn after calcination and after CO hydrogenation in order to determine whether Fe-mixed metal carbides are formed. XANES of principle components (phases) that could possibly be present in Fe catalyst (i.e., Fe_2O_3 , Fe_3O_4 , FeO, Fe_3C , and Fe) were done for a reference purpose and are shown in Figure 6 while Figure 7 shows normalized XANES spectrum of various Fe catalysts with Mn and K promotion.

Initial observation from the XANES shows that all calcined samples have a similar oxidation state (the pre-edge feature shown in Figure 7). Hence, there are no apparent differences in samples after calcination, regardless of whether there is a K chemical promoter or Mn was added to the catalyst. As can be seen in Figure 7, the post-reaction 80Fe20Mn sample was reduced less than the post-reaction 95Fe5Mn sample. This is observed by the slightly lower pre-edge peak (which more resembles Fe_3O_4 rather than Fe_3C). The increase of Mn in the catalyst may reduce Fe_3C formation. While Fe_3C (more specifically any Fe carbide) is likely the active phase in Fe-based Fischer-Tropsch, work by Herrantz et al. [14] shows a mixed metal oxide formed in the presence of sufficient Mn which may cause the slightly less reduced sample.

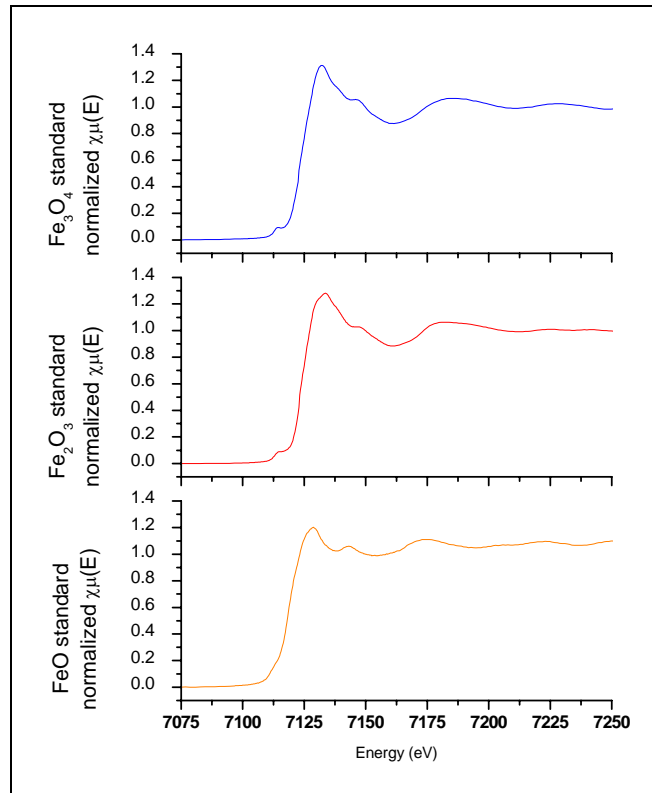


Figure 6: Normalized XANES spectrum of Fe standards

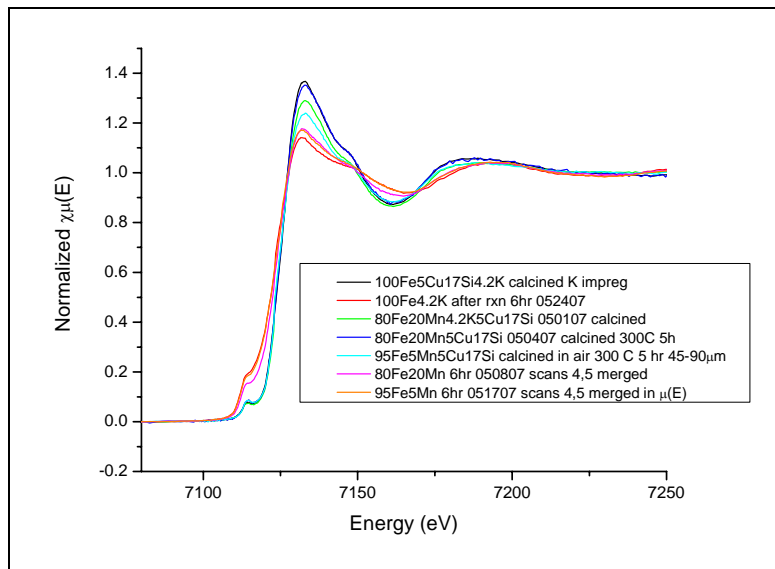


Figure 7: Normalized XANES spectrum of Fe unknowns

A similar treatment for studying the k-edge XANES of Fe will be applied to the k-edge of Mn, by comparing the standards shown in Figure 8 for Mn_2O_3 , MnO , and MnO_2 . Initial comparisons show that there is a broad peak in the XANES region for the post-reaction 80Fe20Mn (Figure 9), indicating that a phase transformation occurred (which resembles none of the standards). It will be necessary to run a series of FEFF 8.4 calculations [15] which simulates the local environment of a specified unit cell and generates an *ab initio* XANES spectrum to determine the structure of the material. The XANES of 95Fe5Mn post-reaction sample is definitively different from the 80Fe20Mn post-reaction sample as well as the standards. However, Herranz et. al. [14] found no evidence of a mixed metal oxide at these metal loadings, a more in depth *ab initio* approach may give more insight into whether a partial mixed metal carbide may be formed.

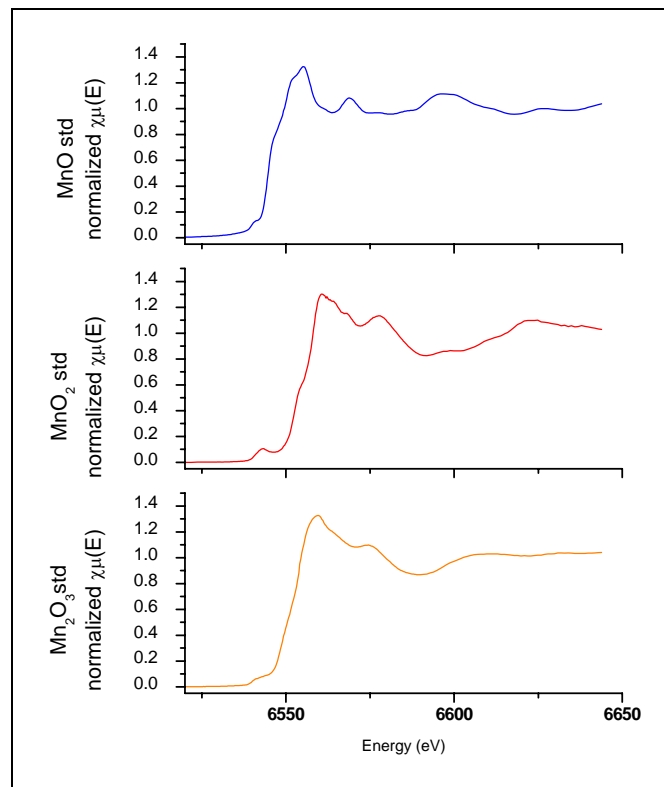


Figure 8: Normalized XANES spectrum of Mn standards

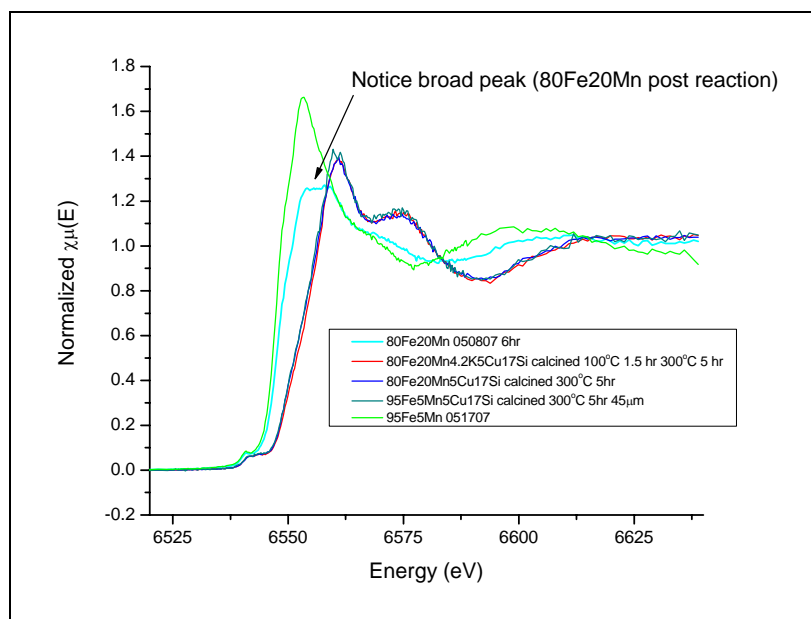


Figure 9: Normalized XANES spectrum of Mn unknowns

3.0 Conclusions

Studies of the impact of different transition metal promotion on Fe catalyst activity were completed. A full manuscript comprising all results will be submitted to a peer-review journal in the field within this month.

4.0 Next Quarter's Activities

Research carried out in the next quarter will be an investigation of the impact of Cr, Mn and Zr addition to the Fe catalyst (shown to exhibit the highest activities) on surface kinetic parameters determined using SSITKA (steady state isotopic transient kinetic analysis). At LSU, FEFF calculations as well as the study of XANES results will be carried out.

References

- [1] D.B. Bukur, X.S. Lang, J.A. Rossin, W.H. Zimmerman, M.P. Rosynek, E.B. Yeh, C.P. Li, *Ind. Eng. Chem. Res.* 28 (1989) 1130.
- [2] K. Sudsakorn, J.G. Goodwin, Jr., A.A. Adeyiga, *J. Catal.* 213 (2003) 204.
- [3] D.B. Bukur, C. Sivaraj, *Appl. Catal. A-Gen.* 231 (2002) 201.
- [4] I.S.C. Hughes, J.O.H. Newman, G.C. Bond, *Appl. Catal.* 30 (1987) 303.
- [5] M.D. Lee, J.F. Lee, C.S. Chang, T.Y. Dong, *Appl. Catal.* 72 (1991) 267.
- [6] H.J. Jung, M.A. Vannice, L.N. Mulay, R.M. Stanfield, W.N. Delgass, *J. Catal.* 76 (1982) 208.
- [7] I.L. Junior, J.M.M. Millet, M. Aouine, M. do Carmo Rangel, *Appl. Catal. A-Gen.* 283 (2005) 91.
- [8] W. Ma, E.L. Kugler, J. Wright, D.B. Dadyburjor, *Energy Fuel* 20 (2006) 2299.

- [9] S. Li, G.D. Meitzner, and E. Iglesia, *J. Phys. Chem. B*, 2001. **105**(24): p. 5743-5750.
- [10] S. Li, G.D. Meitzner, and E. Iglesia, *App. Catal. A: Gen.*, 2001. **219**(1-2): p. 215-222.
- [11] W.D. Callister Jr., *Materials Science and Engineering an Introduction*. Sixth ed. 2003: John Wiley and Sons, Inc. p. 820.
- [12] *X-ray absorption fine structure for catalysts and surfaces*. Series on synchrotron radiation techniques and applications, ed. Y. Iwaswa. Vol. 2. 1996, Tokyo, Japan: World Scientific. 410.
- [13] D.C. Koningsberger and R. Prins, *X-ray absorption : principles, applications, techniques of EXAFS, SEXAFS, and XANES*. 1987, New York: Wiley. xii, 673 p.
- [14] T. Herranz, *J. Catal.* 2006. **243**(1): p. 199-211.
- [15] A.L. Ankudinov, B. Ravel, J.J. Rehr, and S.D. Conradson, *Phys. Rev. B* 58, 7565 (1998).